



Sensitivity of inferred regional CO source estimates

Z. Jiang et al.

This discussion paper is/has been under review for the journal Atmospheric Chemistry and Physics (ACP). Please refer to the corresponding final paper in ACP if available.

Sensitivity of inferred regional CO source estimates to the vertical structure in CO as observed by MOPITT

Z. Jiang^{1,*}, D. B. A. Jones^{1,2}, H. M. Worden³, and D. K. Henze⁴

¹Department of Physics, University of Toronto, Toronto, ON, Canada

²JIFRESSE, University of California, Los Angeles, Los Angeles, CA, USA

³National Center for Atmospheric Research, Boulder, CO, USA

⁴Department of Mechanical Engineering, University of Colorado Boulder, Boulder, CO, USA

*now at: Jet Propulsion Laboratory, California Institute of Technology, Pasadena CA, USA

Received: 8 August 2014 – Accepted: 25 August 2014 – Published: 8 September 2014

Correspondence to: Z. Jiang (zhe.jiang@jpl.nasa.gov)

Published by Copernicus Publications on behalf of the European Geosciences Union.

Title Page

Abstract

Introduction

Conclusions

References

Tables

Figures



Back

Close

Full Screen / Esc

Printer-friendly Version

Interactive Discussion



Abstract

Vertical transport of surface emission to the free troposphere, usually associated with frontal lifting in warm conveyor belts or ascent in deep convection, has significant influence on the vertical structure of atmospheric trace gases. Consequently, it may impact estimates of the surface fluxes of these gases inferred from remote sensing observations that are based on thermal infrared radiances (TIR), since these measurements are sensitive mainly to signals in the free troposphere. In this work, we assessed the sensitivity of regional CO source estimates to the vertical CO distribution, by assimilating multi-spectral MOPITT V5J CO retrievals with the GEOS-Chem model. We compared the source estimates obtained by assimilating the CO profiles and the surface layer retrievals from June 2004 to May 2005. The inversion analyses all produced a reduction in CO emissions in the tropics and subtropics and an increase in the extratropics. The tropical decreases were particularly pronounced for regions where the biogenic source of CO was dominant, suggesting an overestimate of the a priori isoprene source of CO in the model. We found that the differences between the regional source estimates inferred from the profile and surface layer retrievals for 2004–2005 were small, generally less than 5% for the main continental regions, except for estimates for South Asia, North America, and Europe. Because of discrepancies in convective transport in the model, the CO source estimates for India and Southeast Asia inferred from the CO profiles were significantly higher than those estimated from the surface layer retrievals during June–August 2004. On the other hand, the profile inversion underestimated the CO emissions from North America and Europe compared to the assimilation of the surface layer retrievals. We showed that vertical transport of air from the North American and European boundary layer is slower than from other continental regions and thus air in the free troposphere from North America and Europe is more chemically aged, which could explain the discrepancy between the source estimates inferred from the profile and surface layer retrievals. We also examined the impact of the OH distribution on the source estimates using OH fields from versions v5-07-08 and v8-02-

Sensitivity of inferred regional CO source estimates

Z. Jiang et al.

Title Page

Abstract

Introduction

Conclusions

References

Tables

Figures



Back

Close

Full Screen / Esc

Printer-friendly Version

Interactive Discussion



Sensitivity of inferred regional CO source estimates

Z. Jiang et al.

Title Page

Abstract

Introduction

Conclusions

References

Tables

Figures



Back

Close

Full Screen / Esc

Printer-friendly Version

Interactive Discussion



01 of GEOS-Chem. The impact of the different OH fields was particularly large for the extratropical source estimates. For example, for North America, using the surface layer retrievals, we estimated a total CO source of 37 and 55 Tg CO with the v5-07-08 and v8-02-01 OH fields, respectively, for June–August 2004. For Europe the source estimates were 57 and 72 Tg CO, respectively. We found that the discrepancies between the source estimates obtained with the two OH fields were larger when using the profile data, which is consistent with greater sensitivity to the more chemically aged air in the free troposphere. Our findings indicate that regional CO source estimates are sensitive to the vertical CO structure. They suggest that assimilating a broader range of composition measurements to provide better constraint on tropospheric OH and the biogenic sources of CO is essential for reliable quantification of the regional CO budget.

1 Introduction

The emissions of greenhouse gases and other atmospheric pollutants have been significantly increased since the industrial revolution. Their influences on atmospheric chemical composition, local air quality and climate are the subject of increasing numbers of studies. In this context, inverse modeling has been widely used to provide better understanding of the emissions of these atmospheric constituents. In particular, in the past decade there has been expanded use of inverse modeling to better quantify the emissions of atmospheric CO (Pétron et al., 2004; Heald et al., 2004; Arellano et al., 2006; Jones et al., 2009; Kopacz et al., 2010; Fortems-Cheiney et al., 2011; Gonzi et al., 2011). Tropospheric CO is produced from incomplete combustion and is a byproduct of oxidation of hydrocarbons. As the primary sink of OH, tropospheric CO has significant influence on the oxidative capacity of the atmosphere. The lifetime of tropospheric CO is a few months, which is long enough to track within intercontinental scale pollution plumes but short enough to provide strong signals over background distribution (Jiang et al., 2010). Previous studies (Palmer et al., 2006; Wang et al., 2009)

have demonstrated that CO can be included in the inverse analyses of CO₂ to reduce the influence of model transport errors.

Remote sensing from space-based instruments provide valuable global observational coverage to enable us to better constrain CO emission. There are now several satellite sensors from which abundances of CO in the troposphere have been retrieved using measurement of thermal infrared (TIR) radiation near 4.7 μm: MOPITT, on EOS-Terra, was launched December 1999 (Deeter et al., 2003), AIRS, on EOS-Aqua, was launched May, 2002 (Warner et al., 2007), TES, on EOS-Aura, was launched July, 2004 (Luo et al., 2007), and IASI (the Infrared Atmospheric Sounding Interferometer), on METOP-A, was launched October, 2006 (George et al., 2009). The TIR radiances are sensitive to CO concentrations from the middle to the upper troposphere. The lack of global observations of CO near the surface has implications for the use of inverse modeling to quantify CO emissions because CO signals in the free troposphere are affected by discrepancies in the parameterization of convective transport, the chemical sink of CO, and in long-range transport in models (e.g. Arellano et al., 2006b; Jiang et al., 2013).

The multispectral MOPITT version 5 CO product (V5J, where J indicates joint retrievals) are the first retrievals to exploit simultaneous near infrared (NIR) and TIR measurement to provide greater sensitivity to lower tropospheric CO signals over land (Deeter et al., 2011). Recently, Jiang et al. (2013) showed that lower tropospheric MOPITT V5J CO retrievals can be used to study the influence of convective transport error on CO source estimates. They compared the CO source estimates in June–August 2006, inferred from MOPITT surface layer retrievals, the profile retrievals, and the column amounts. They found that there were large discrepancies in the inferred source estimates obtained with the surface layer and profile retrievals in Asian monsoon regions where strong emissions are co-located with significant vertical mass flux due to convection. The discrepancies in the CO source estimates were also used to assess the impact of vertical transport error on the CH₄ emission estimates from Indonesian peat fires in fall 2006, estimated from TES CH₄ observations (Worden et al., 2013).

Sensitivity of inferred regional CO source estimates

Z. Jiang et al.

Title Page

Abstract

Introduction

Conclusions

References

Tables

Figures



Back

Close

Full Screen / Esc

Printer-friendly Version

Interactive Discussion



equator at 10:30 local time. With a footprint of 22 km × 22 km, the instrument makes measurements in a 612 km cross-track scan that provides global coverage every three days. The MOPITT data used here were obtained from the joint retrieval of CO from TIR (4.7 μm) and NIR (2.3 μm) radiances using an optimal estimation approach (Worden et al., 2010; Deeter et al., 2011). The retrieved volume mixing ratios (VMR) are reported for the layer average above 10 pressure levels (surface, 900, 800, 700, 600, 500, 400, 300, 200 and 100 hPa) and the relationship between the retrieved CO profile and the true atmospheric state can be expressed as:

$$\hat{\mathbf{Z}} = \mathbf{Z}_a + \mathbf{A}(\mathbf{Z} - \mathbf{Z}_a) + \mathbf{G}\varepsilon \quad (1)$$

where \mathbf{Z}_a is the MOPITT a priori CO profile (expressed as log(VMR)), \mathbf{Z} is the true atmospheric state (also as log(VMR)), $\mathbf{G}\varepsilon$ describes the retrieval error, and $\mathbf{A} = \partial\hat{\mathbf{A}}/\partial\mathbf{Z}$ is the MOPITT averaging kernel matrix, which gives the sensitivity of the retrieval to the actual CO in the atmosphere. The MOPITT V5 data have been evaluated by Deeter et al. (2012, 2013) using aircraft measurements from the National Oceanic and Atmospheric Administration (NOAA). For the V5J multi-spectral retrievals, they found a small positive bias of 2.7% at the surface and a much larger positive bias of 14% at 200 hPa. As a result of the high bias in the upper troposphere, in our analysis we do not use the retrievals at altitudes above 200 hPa. An indirect validation presented in Section 4.1, using NOAA GMD in situ observations, suggests a high-latitude positive bias in the MOPITT data, partially associated with the lower degrees-of-freedom-for-signal (DFS) at higher latitudes. Consequently, in this work, we omitted MOPITT data that are polarward of 40° over oceans and 52° over land.

2.2 GEOS-Chem

The GEOS-Chem global chemical transport model (CTM) www.geos-chem.org is driven by assimilated meteorological observations from the NASA Goddard Earth Observing System (GEOS-5) at the Global Modeling and data Assimilation Office. We

Sensitivity of inferred regional CO source estimates

Z. Jiang et al.

Title Page

Abstract

Introduction

Conclusions

References

Tables

Figures



Back

Close

Full Screen / Esc

Printer-friendly Version

Interactive Discussion



Sensitivity of inferred regional CO source estimates

Z. Jiang et al.

use version v34 of the GEOS-Chem adjoint, which is based on v8-02-01 of the forward GEOS-Chem model, with relevant updates through v9-01-01. Our analysis is conducted at a horizontal resolution of $4 \times 5^\circ$ and employs the CO-only simulation in GEOS-Chem, which uses archived monthly OH fields from the full chemistry simulation. The standard OH field used in this work is from GEOS-Chem version v5-07-08, with a global annual mean OH concentration of $0.99 \times 10^6 \text{ molec cm}^{-3}$ (Evans et al., 2005). We use this as our standard OH field to facilitate comparison of our results with those of Kopacz et al. (2010). We also conduct a sensitivity analysis using OH fields from the full chemistry simulation of v34 of the adjoint model, run in forward mode. This simulation produces a global annual mean OH concentration of $1.24 \times 10^6 \text{ molec cm}^{-3}$.

The anthropogenic emission inventories are identical to those used in Jiang et al. (2013). Anthropogenic emissions are from EDGAR 3.2FT2000 (Olivier et al., 2001), but are replaced by the following regional emission inventories: the US Environmental Protection Agency National Emission Inventory (NEI) for 2005 in North America, the Criteria Air Contaminants (CAC) inventory for Canada, the Big Bend Regional Aerosol and Visibility Observational (BRAVO) Study Emissions Inventory for Mexico (Kuhns et al., 2003), the Cooperative Program for Monitoring and Evaluation of the Long-range Transmission of Air Pollutants in Europe (EMEP) inventory for Europe in 2000 (Vestreng et al., 2002) and the INTEX-B Asia emissions inventory for 2006 (Zhang et al., 2009). Biomass burning emissions are based on the Global Fire Emission Database (GFED3), with a three-hour temporal resolution (van der Werf et al., 2010). Additional CO sources come from oxidation of methane and biogenic volatile organic compounds (VOCs,) as described in previous studies (Kopacz et al., 2010; Jiang et al., 2013). The distribution of the annual mean CO emissions for June 2004 to May 2005 is shown in Fig. 1. The annual global sources are 928 Tg CO from fossil fuel, biofuel and biomass burning, 661 Tg CO from the oxidation of biogenic NMVOCs, and 884 Tg CO from the oxidation of CH_4 .

[Title Page](#)[Abstract](#)[Introduction](#)[Conclusions](#)[References](#)[Tables](#)[Figures](#)[Back](#)[Close](#)[Full Screen / Esc](#)[Printer-friendly Version](#)[Interactive Discussion](#)

3 Inversion approach

We use the 4-dimensional variational (4D-var) data assimilation system in GEOS-Chem (e.g., Henze et al., 2007; Kopacz et al., 2009, 2010; Singh et al., 2011; Jiang et al., 2011, 2013; Parrington et al., 2012) to estimate the CO sources. In this approach, we minimize the cost function of the form,

$$J(\mathbf{x}) = (\mathbf{F}(\mathbf{x}) - \mathbf{y})^T \mathbf{S}_{\Sigma}^{-1} (\mathbf{F}(\mathbf{x}) - \mathbf{y}) + (\mathbf{x} - \mathbf{x}_a)^T \mathbf{S}_a^{-1} (\mathbf{x} - \mathbf{x}_a) \quad (2)$$

where \mathbf{x} is the state vector of CO emissions, N is the number of observations that are distributed in time over the assimilation period, \mathbf{y}_i is a vector of observed concentrations at a given time, and $\mathbf{F}(\mathbf{x})$ is the forward model which represents the transport of the CO emissions in the GEOS-Chem model and accounts for the vertical smoothing of the MOPITT retrieval, \mathbf{x}_a is the a priori estimate, and \mathbf{S}_{Σ} and \mathbf{S}_a are the observational and a priori error covariance matrices, respectively.

For the results presented here, the state vector in Eq. (2) is not the CO emissions, but is a set scaling factors s such that $\mathbf{x} = \sigma \mathbf{x}_a$. Consequently, the optimization is conducted by minimizing the gradient of the cost function with respect to the scaling factors, with errors in the emission inventories assumed on a relative basis rather than on an absolute basis. In this approach, the gradient of the cost function as described in Eq. (2) is usually scaled as follows:

$$\frac{\partial J}{\partial(\mathbf{x}/\mathbf{x}_a)} = \frac{\partial J}{\partial \mathbf{x}} \cdot \mathbf{x}_a \quad (3)$$

This method is referred to as the linear scaling factor optimization. It assumes that the uncertainty in the emissions is normally distributed about scaling factor one. Henze et al. (2009) indicated that the normal distribution about one is nonphysical because it allows the negative emissions. An alternative method is the logarithm (LOG) scaling factor optimization (Henze et al., 2009):

$$\frac{\partial J}{\partial \ln(\mathbf{x}/\mathbf{x}_a)} = \frac{\partial J}{\partial \mathbf{x}} \cdot \mathbf{x}_a \cdot \frac{\mathbf{x}}{\mathbf{x}_a} \quad (4)$$

Sensitivity of inferred regional CO source estimates

Z. Jiang et al.

Title Page

Abstract

Introduction

Conclusions

References

Tables

Figures



Back

Close

Full Screen / Esc

Printer-friendly Version

Interactive Discussion



Sensitivity of inferred regional CO source estimates

Z. Jiang et al.

Title Page

Abstract

Introduction

Conclusions

References

Tables

Figures



Back

Close

Full Screen / Esc

Printer-friendly Version

Interactive Discussion



It represents a log-normal distribution of scaling factors about zero. One advantage of LOG scaling factor optimization is that it can prevent negative scaling factors (Henze et al., 2009). However, it does not reduce negative gradients effectively because the increase in the factor x/x_a will partially offset the decrease of $\partial J/\partial x$. Figure 2 shows the results of linear scaling optimization and the LOG optimization in an OSSE for April 2006. In the OSSE, we firstly create pseudo-observations, by archiving model output with CO emission unchanged. In the pseudo-inversion, we reduced the CO emission by 50% and the objective of the OSSE is to observe whether the scaling factors can return to true state (1.0). After 30 iterations, the a posteriori estimate with linear method (Fig. 2a) converged to true state in all major emission regions. The results with LOG method are clearly worse (Fig. 2b).

To better reduce the negative gradient, and avoid negative scaling factors, we developed the following modification to the LOG method:

$$\frac{\partial J}{\partial \ln(x/x_a)} = \frac{\partial J}{\partial x} \cdot x_a \cdot \frac{x}{x_a} \text{ when: } \frac{x}{x_a} \leq 1$$

$$\frac{\partial J}{\partial \frac{1}{2}[(x/x_a)^2 - 1]} = \frac{\partial J}{\partial x} \cdot x_a / \frac{x}{x_a} \text{ when: } \frac{x}{x_a} > 1 \quad (5)$$

This new method is referred to as “LOGX2”. It can minimize the positive and negative gradients with comparable efficiency. As shown in Fig. 2c, the optimization effect of the LOGX2 method is slightly better than that of the linear method. However, it should be noted that although the LOGX2 approach improves the optimization efficiency and minimizes the potential systematic errors, it impacts the statics of the solution. With the linear or LOG approaches the errors are Gaussian or log-normal, respectively, but with the LOGX2 scheme they are neither.

We employ a similar procedure for data processing and quality control as in our previous study, Jiang et al. (2013). Since MOPITT V5J CO retrievals have a positive bias at high altitudes (Deeter et al., 2013), our analysis is restricted to CO retrievals below 200 hPa. We also reject MOPITT data with CO column amounts less than 5×10^{17}

molec/cm² and use only daytime data. Following Jiang et al. (2011, 2013), we assume a uniform observation error of 20%. The observation error is meant to represent the retrieval errors, representativeness errors, and the influence of random errors in the model. Using the Relative Residual Error approach (Palmer et al., 2003; Heald et al., 2004), which assumes that the mean differences between the model and observations are due to discrepancies in the emissions while the residual reflects the observation error, Kopacz et al. (2010) estimated that the observation errors for the MOPITT columns are 10–30%. Our assumed 20% error likely overestimates the observation error in the upper troposphere and underestimates it near the surface. As noted in Jiang et al. (2013), we expect this assumption of a uniform observation error to have a negligible impact on our inversion results.

As described in Jiang et al. (2013), we combine the combustion CO sources (fossil fuel, biofuel and biomass burning) with the CO from the oxidation of biogenic NMVOCs and solve for the total CO emissions in each grid box, assuming a 50% uniform a priori error and that the errors are uncorrelated. We optimize the source of CO from the oxidation of methane separately as an aggregated global source, assuming an a priori uncertainty of 25%. As in Jiang et al. (2013), we produce initial conditions at the beginning of each monthly assimilation window by assimilating MOPITT V5J data using a sequential sub-optimal Kalman filter (Parrington et al., 2008). For the results presented here, the Kalman filter assimilation was carried out from 1 January 2004, to 1 May 2005, and the optimized initial conditions were archived at the beginning of each month. Consequently, the initial conditions for the model simulation are independent of the inverse analyses. Although we use a one-month assimilation window, it is possible that a longer window of two or three months would lead to greater constraints on the CO source estimates. However, as we will shown below, the inversion is sensitive to the specified OH distribution and thus with a longer assimilation window we would be more susceptible to discrepancies in the CO chemical sink.

Sensitivity of inferred regional CO source estimates

Z. Jiang et al.

[Title Page](#)[Abstract](#)[Introduction](#)[Conclusions](#)[References](#)[Tables](#)[Figures](#)[Back](#)[Close](#)[Full Screen / Esc](#)[Printer-friendly Version](#)[Interactive Discussion](#)

4 Results and discussion

4.1 Indirect Validation of the MOPITT V5J Data

Although Deeter et al. (2012, 2013) showed that the bias in the V5 MOPITT data relative to aircraft observation is small in the lower troposphere, we note that the aircraft data are limited in space and time. Therefore, here we conduct an indirect validation of the MOPITT data by assimilating the data to optimize the modeled CO distribution and compare it with independent data. A better understanding of potential bias in the data is critical for properly quantifying the source estimates. Comparison of the CO distribution obtained with the a posteriori source estimates can reveal potential bias in the inversion, but in that approach it is difficult to determine whether the bias is in the data or the model. By constraining the modeled CO to match the observations, we can more easily identify potential biases in the data. For example, recent inversion studies (Arellano et al., 2006; Jones et al., 2009; Hooghiemstra et al., 2012) have shown that the a posteriori CO emissions, inferred from MOPITT data, resulted in an overestimate of CO abundances relative to surface in situ measurements. Hooghiemstra et al. (2012) suggested that the overestimate of surface CO was due to a bias in the V4 MOPITT data that they employed. However, Arellano et al. (2006) and Jones et al. (2009) used the V3 MOPITT product in their inversion analyses. Jiang et al. (2013) suggested that the bias seen by Hooghiemstra et al. (2012) could be due to discrepancies in vertical transport. We also note that MOPITT validation comparisons (Deeter et al., 2010; 2013) over land rely on NOAA aircraft in situ CO profiles that are concentrated in North America with only 2 out of 15 locations at latitudes higher than 50° N.

To assess potential bias in the MOPITT data set, we assimilated the MOPITT V5J CO profile data into the GEOS-Chem model using the sequential sub-optimal Kalman filter and compare the resulting CO field with GMD in situ surface CO observations. Figure 3 shows the comparison of the assimilated CO with monthly mean CO concentrations at selected GMD sites. In the Northern Hemisphere, the CO concentration of the free run model, with original initial condition, is higher than that of GMD in summer

Sensitivity of inferred regional CO source estimates

Z. Jiang et al.

Title Page

Abstract

Introduction

Conclusions

References

Tables

Figures



Back

Close

Full Screen / Esc

Printer-friendly Version

Interactive Discussion



Sensitivity of inferred regional CO source estimates

Z. Jiang et al.

Title Page

Abstract

Introduction

Conclusions

References

Tables

Figures



Back

Close

Full Screen / Esc

Printer-friendly Version

Interactive Discussion



and fall, and significantly lower than that of GMD in winter and spring. In the Southern Hemisphere, the free run model generally overestimates the observed CO, which is consistent with previous studies (Shindell et al., 2006; Kopacz et al., 2010). In our assimilation, we first assimilated the MOPITT data between 60° S to 60° N. The result shows that assimilated MOPITT data (dark blue dotted line) are highly consistent with the GMD data between 0° N to 30° N. However, the analysis has a positive bias in the mid-latitudes of the Southern Hemisphere and in the high latitudes of the north hemisphere, such as at Cold Bay (CBA), Alaska, and Mace Head (MHD), Ireland. At CBA and MHD the free running model (the a priori) overestimated the observed CO between August–November 2004, but underestimated it at CBA between January–March 2005. At MHD the a priori agreed well with the data during the latter half of the assimilation period. In contrast, at both sites the assimilated CO is biased high throughout the year, suggesting a high latitude bias in the MOPITT data. In the Southern Hemisphere, at Crozet Island (CGO), the a priori is bias high and the assimilation exacerbated the bias, which supports the conclusion of Hooghiemstra et al. (2012) that the MOPITT data are biased high in the Southern Hemisphere. To reduce the potential impact of this high latitude bias in both hemispheres, we omitted MOPITT data in the assimilation that are polarward of 40° over oceans and 52° over land. As shown in Fig. 3, this improved the agreement between the assimilated CO and the GMD data, but it did not completely remove the positive high-latitude bias at MHD and CGO. The results in Fig. 3 show the value in the optimized initial conditions prior to the source estimation. The initial condition biases are much smaller than using original initial conditions from the free running model, particularly in winter and spring.

To assess the potential impact of the high latitude bias on the source estimates, we conducted one inversion analysis using the MOPITT data between 60° S–60° N and one with the data between 40° S–40° N over oceans and between 52° S–52° N over land. Figure 4 shows the CO emission scaling factors obtained with and without the additional high latitude MOPITT data, using MOPITT surface layer retrievals. The impact in the Southern Hemisphere is negligible since there are few CO sources in the

middle and high latitudes of the Southern Hemisphere, and also because the retrieval in the lower troposphere, over oceans, is only weakly sensitive to CO (due to the lack of NIR information). Consequently, we expect that our a posteriori CO emissions produce an overestimate in CO in the Southern Hemisphere. In the Northern Hemisphere, the additional high latitude MOPITT data leads to larger emission estimates at high latitudes and smaller estimates at middle latitudes. Since we have not fully mitigated this high latitude bias, we note that our inversion results presented below will reflect the influence of this bias.

4.2 CO Source Estimates for June 2004–May 2005

Figure 5a and b show the annual mean emission scaling factors for June 2004 to May 2005, obtained using the MOPITT surface layer and profile retrievals, respectively. Both analyses suggest that CO emissions in the tropics should be reduced, whereas the emissions in middle and high latitudes should be increased. However, as shown in Fig. 5c, the a posteriori emissions from profile inversion is higher in India and Southeast Asia. As discussed in Jiang et al. (2013), these discrepancies over India and Southeast Asia are likely due to model errors in convection transport. The profile inversion also produces larger emissions in parts of tropical Africa and northern South America. In general, however, the a posteriori emissions from the profile inversion are lower than those obtained from the surface layer inversion, particularly at middle and high latitudes.

Table 1 shows the annual mean regional CO emissions from June 2004 to May 2005, inferred from the surface layer and profile retrievals. In this work, only the total CO emission is optimized in each grid box, but because the different CO source types have different spatial and temporal distributions, we apply the scaling factors in each grid box to each source type, which can provide useful information on the individual source types. As shown in Table 1, the emission reductions in the tropics and subtropics reflect large reductions in the biogenic source of CO, suggesting that our a priori biogenic emissions are too high. For example, in South America, with the pro-

Sensitivity of inferred regional CO source estimates

Z. Jiang et al.

Title Page

Abstract

Introduction

Conclusions

References

Tables

Figures



Back

Close

Full Screen / Esc

Printer-friendly Version

Interactive Discussion



Sensitivity of inferred regional CO source estimates

Z. Jiang et al.

file inversion the biogenic source was reduced 32 %, whereas the combustion source was reduced by 13 %. In northern Africa the biogenic source was reduced by 26 % and the combustion source was reduced by 20 % with the profile inversion. In the 48 contiguous United States the biogenic source was reduced by 31 %, whereas the combustion source was increased by 5 %. The reductions in the biogenic emissions were smaller in the surface layer inversion, but were still large for South America and northern Africa, 27 and 28 %, respectively. We note that although there are large differences between the regional source estimates inferred from the profile and surface layer retrievals, the global total a posteriori CO emissions from two inversions are similar, 1513 and 1555 Tg CO, respectively.

The seasonal mean scaling factors are shown in Fig. 6. The main seasonal feature in the figure is that the inversions tend to decrease CO emission in the summer hemisphere and increase them in the winter hemisphere, with the profile inversion producing larger reductions (Fig. 6a and b) and smaller increases (Fig. 6c and g). Consequently, the differences between the scaling factors from the surface and profile inversions are smaller in winter. This pattern is consistent with an overestimate of isoprene emissions and a possible underestimate of wintertime fossil fuel combustion. It is also possible that the modeled OH fields are biased high in summer, when the CO lifetime is short. However, the overestimate of biogenic emissions in GEOS-Chem by the Model of Emissions of Gases and Aerosols from Nature (MEGAN) has been reported by previous studies (Barkley et al., 2008; Millet et al., 2008; Liu et al., 2010). Millet et al. (2008) found that North American isoprene emissions estimated by MEGAN were greater than those inferred from observations of formaldehyde (HCHO) from the Ozone Monitoring Instrument (OMI) by as much as 23 %. Liu et al. (2010) used a newer version of MEGAN, version 2.1, which simulates lower isoprene emissions than version 2.0 (which is employed in our analysis), and found that it also produced an overestimate of CO from isoprene oxidation, particularly in eastern South America. This is an issue because they showed that although biomass burning is the dominant CO signal in the lower troposphere over South America in summer and fall (July–October), during the

[Title Page](#)[Abstract](#)[Introduction](#)[Conclusions](#)[References](#)[Tables](#)[Figures](#)[Back](#)[Close](#)[Full Screen / Esc](#)[Printer-friendly Version](#)[Interactive Discussion](#)

Sensitivity of inferred regional CO source estimates

Z. Jiang et al.

Title Page

Abstract

Introduction

Conclusions

References

Tables

Figures



Back

Close

Full Screen / Esc

Printer-friendly Version

Interactive Discussion



50 % larger than the summer emissions, whereas our winter emissions were about a factor of 2–3 time larger than our summer estimates. As a result, our annual combustion emission estimate for the contiguous United States was 100 Tg from the profile inversion, whereas Kopacz et al. (2010) inferred 50 Tg. A significant difference between our inversion and that of Kopacz et al. (2010) is that their a priori combustion source for the United States was 40 Tg, whereas ours was 112 Tg. Their low a priori estimate was based on the results of Hudman et al. (2008), who suggested a 60 % reduction in anthropogenic emissions in the United States as a result of an analysis of aircraft data in July–August 2004. The summertime estimates obtained here, as well as those of Kopacz et al. (2010), support the analysis of Hudman et al. (2008). For Europe and East Asia, we also obtained large differences relative to Kopacz et al. (2010). Our inferred a posteriori combustion estimates from the profile inversion were 126 and 233 Tg, for Europe and East Asia, respectively. For comparison, Kopacz et al. (2010) inferred a posteriori estimates of 95 Tg and 354 Tg, respectively, for these regions.

Despite the large differences between the region source estimates inferred here and those from Kopacz et al. (2010), there is good agreement between the two studies in the aggregated emissions in the extratropical Northern Hemisphere. The total combined a posteriori combustion source from the United States, Alaska, Canada, Europe, and East Asia was 515 and 548 Tg from the profile and surface inversions, respectively. The corresponding a posteriori estimate from Kopacz et al. (2010), was 520 Tg. Kopacz et al. (2010) used data from MOPITT, SCIAMACHY, and AIRS, so the agreement in the aggregated estimates suggests that the data are providing consistent information on the extratropical Northern Hemisphere combustion source, but there are discrepancies in the regional partitioning of this information in the inversions. These discrepancies could be related to differences in configuration of the inversion analyses, such as the treatment of the initial conditions or vertical transport in the models. Our inversion analyses employed the GEOS-5 meteorological fields, whereas Kopacz et al. (2010) used GEOS-4. A significant factor could be the treatment of the biogenic source of CO. Here the the biogenic source are combined with the combustion sources and optimize at

the resolution of the model. In contrast, Kopacz et al. (2010) aggregated the biogenic source with the methane source and optimize the global mean source from methane and VOC oxidation. As shown in Jiang et al. (2011), optimizing the VOC source at a lower resolution than the combustion emissions could result in an overadjustment of the combustion sources.

In general, we find that the regional source estimates inferred from the surface layer and profile retrievals are consistent, with relative differences of less than 10 %, except for source estimates for North America (the United States, Alaska and Canada), Europe, and India/southeast Asia (see Table 1). The relative differences in the CO column abundances simulated with the a posteriori CO estimates, shown in Fig. 8, are also small, except over the main source regions, such as eastern North America. As discussed above, the difference between the two inversions in the extratropical Northern Hemisphere are larger in summer than in winter. The pronounced discrepancy between the two inversions over India/southeast Asia in summer is linked to vertical transport by the Asian monsoon and was discussed by Jiang et al. (2013). We note that between June - August 2004, the CO columns simulated from the profile inversion a posteriori source estimates are lower than those from the surface layer inversion globally, except over India/southeast Asia. This is in contrast to Jiang et al. (2013), who found that their MOPITT profile inversion produced larger CO column abundances than their surface layer inversion for June–August 2006. We believe that this difference is due, in part, to the different OH fields used in here and in Jiang et al. (2013) (as will be discuss in the next section), and also to the fact that deep convection over India and southeast Asia was much stronger in June–August 2006 than in June–August 2004. Figure 8 also shows that the consistency between the a posteriori annual mean source estimates for South America from the profile and surface inversions reflect compensating discrepancies. The profile inversion produced larger a posteriori CO columns between September – December 2004 and smaller CO columns during the rest of the year. These difference may be due to changes in the relative contribution from the biogenic

Sensitivity of inferred regional CO source estimates

Z. Jiang et al.

[Title Page](#)[Abstract](#)[Introduction](#)[Conclusions](#)[References](#)[Tables](#)[Figures](#)[Back](#)[Close](#)[Full Screen / Esc](#)[Printer-friendly Version](#)[Interactive Discussion](#)

and biomass burning sources in South America and the influence of vertical transport associated with the seasonal variations in the Intertropical Convergence Zone (ITCZ).

4.3 Ideal Tracer Experiments

It is surprising that Europe and North America (The United States and Canada) are the two regions, after India/southeast Asia, with the largest discrepancies between the source estimates inferred from the profile and surface layer inversions. To better understand how the vertical transport of CO from these region could impact the inversions, we conducted an analysis using an idealized CO-like tracer. We performed a tagged-CO simulation for the period June 2004 – May 2005 in which we imposed a constant source of CO of 3.33 Tg CO/day from each of the continental source regions shown in Fig. 9, with a constant and uniform loss frequency of $1/30 \text{ days}^{-1}$. We ran separate tracers for each of the continental regions shown in Fig. 9, with each tracer emitted only in that region but chemically destroyed everywhere. The tracers were initialized to a uniformly low abundance of 1 pptv and the model was run for 17 months prior to June 2004 to spinup the tracer distributions. Shown in Fig. 10 are the boundary layer (defined here as the surface – 700 hPa) and free tropospheric (700–250 hPa) partial columns of the continental tracers for June 2004. In the extratropical Northern Hemisphere, a larger fraction of the Asian surface emissions are exported to the free troposphere, compared to the North American and European emissions. We find that transport of the Asian emissions to the free troposphere is faster even in winter. In the tropics, transport of surface emissions to the free troposphere is slowest for South America (Fig. 10b), most likely due to the fact that in boreal summer the ITCZ is located in northern South America (in the Northern Hemisphere) so transport of south American emissions to the southern subtropics and extratropics is facilitated instead by the influence of mid-latitude cyclones (Staudt et al., 2002). In fall, the ITCZ moves south and convection over South America intensifies (Liu et al., 2010), as a result, we find that, in December, the fraction of South American emissions in the free troposphere is greater, and is comparable to that from northern Africa.

22956

ACPD

14, 22939–22984, 2014

Sensitivity of inferred regional CO source estimates

Z. Jiang et al.

Title Page

Abstract

Introduction

Conclusions

References

Tables

Figures

◀

▶

◀

▶

Back

Close

Full Screen / Esc

Printer-friendly Version

Interactive Discussion



Sensitivity of inferred regional CO source estimates

Z. Jiang et al.

Title Page

Abstract

Introduction

Conclusions

References

Tables

Figures



Back

Close

Full Screen / Esc

Printer-friendly Version

Interactive Discussion



The monthly mean fraction of the global mass of each continental tracer that is in the boundary layer and the free troposphere is listed in Table 2. North America and Europe have the smallest mass fraction in the free troposphere, 26 and 21 %, respectively. This suggests that, relative to the other continental regions, the air in the free troposphere from Europe and North America is older and more chemically aged. Consequently, the surface layer and profile inversions are sampling sufficiently different air masses that they obtain different constraints on the North American and European source estimates. It is possible that a longer assimilation window would lead to more consistent constraints on the source estimates between the surface layer and profile inversions. However, as noted above, with a longer assimilation window the inferred source estimates would be more susceptible to discrepancies in the OH abundance.

4.4 Influence of the OH distribution

In this section we compare the impact on the source estimates of the OH distribution from v8-02-01 of GEOS-Chem with that from our standard inversion (which is based on v5-07-08 of GEOS-Chem). As shown in Fig. 11, v8-02-01 OH is significantly higher than on v5-07-08 in Northern hemisphere, while it is much lower over South America and Indonesia.

Using the v8-02-01 OH fields, we repeated the profile and surface inversions for June–August 2004. Shown in Fig. 12 are the scaling factors and their differences, by using two versions of OH fields. With v8-02-01 OH the a posteriori emissions in the tropics changed only slightly, while the inferred emission estimates in the extratropics, mainly for North America and Europe, were much greater than those obtained with v5-07-08 OH. The regional source estimates are given in Table 3. For the contiguous United States, with v5-07-08 OH we inferred a June–August source of 25.4 Tg using the profile retrievals, whereas with v8-02-01 OH we estimated a source of 49.2 Tg. Similarly, for Europe the source estimates inferred from the profile inversion with v5-07-08 OH was 47.3 Tg, whereas with v8-02-01 OH it with was 68.3 Tg.

5 Summary

We presented a global inversion analysis to quantify monthly mean CO source estimates during the period of June 2004–May 2005 using the version 5 MOPITT retrievals. Building on the work of Jiang et al. (2013), we conducted a comparative analysis of the influence of the MOPITT profile and surface layer retrievals on the inferred CO source estimates. The inversions suggest a reduction in CO emission in the tropics, possible due to an overestimate of the biogenic source of CO, and an increase in emissions at middle and high latitudes. In the northern extratropics, we find that the inferred source estimates are typically much greater in winter than in summer, consistent with the seasonality in CO emissions inferred by Kopacz et al. (2010). With our standard OH distribution, we inferred source estimates of 148, 180, and 284 Tg for the contiguous United States, Europe, and East Asia, respectively, using the surface layer retrievals. Using the profile retrievals, the inferred source estimates were lower, 131, 158, and 282 Tg, respectively. In the tropics, the a posteriori source estimates inferred from the surface layer retrievals for South America, Northern Africa, and Southern Africa were 237, 199, and 170 Tg, compared to the a priori of 298, 247, and 194 Tg, respectively.

In general, we found that the annual mean, regional source estimates inferred from the surface layer retrievals and those from the profile retrievals were in agreement to better than 10%, with the exception of the North American (United States and Canada), European, and Indian/southeast Asian estimates. The difference in the Indian/southeast Asian estimates is due to discrepancies in vertical transport associated with the strong convective transport over the Southeast Asian region (Jiang et al., 2013). For Europe and North America, we argue that the differences in the source estimates from the profile and surface inversion are due to model discrepancies in the free tropospheric abundance of CO from these regions. We conducted an ideal tracer experiment and showed that transport of surface emissions from Europe and North America to the free troposphere is slower than from other continental regions. Consequently, compared to the inversion using the surface layer retrievals, the profile

Sensitivity of inferred regional CO source estimates

Z. Jiang et al.

Title Page

Abstract

Introduction

Conclusions

References

Tables

Figures



Back

Close

Full Screen / Esc

Printer-friendly Version

Interactive Discussion



inversion is sampling older, more chemically aged air from North America and Europe, and is, therefore, more susceptible to discrepancies in long-range transport and in the chemical sink of CO.

We examined the impact of the OH distribution on the inferred CO source estimates, using OH fields from versions v5-07-08 and v8-02-01 of GEOS-Chem. We found that changing OH from v5-07-08 (used in our standard inversions) to v8-02-01 produced large differences in the extratropical source estimates. The relative differences in the source estimates from the profile inversion using v5-07-08 and v8-02-01 OH were 64, 33, and 36 % for source estimates from the contiguous United States, East Asia, and Europe for June–August 2004, when the CO lifetime is short. In the inversions using the surface layer data we found that the impact of the OH fields was reduced, but was still large: 40, 20, and 24 %, respectively. The smaller impact of the OH fields in the surface layer inversion is due to the fact that the OH sink is at a maximum in the middle troposphere, while the surface layer retrievals have maximum sensitivity near the boundary layer.

The results presented here clearly demonstrate the challenge of inverse modeling of CO emissions. Although the CO chemistry is relatively simple, the sensitivity to tropospheric OH is a major issue. Accurate OH fields are essential for constraining CO reliably. In recent studies, Fortems-Cheiney et al. (2011) introduced Methyl Chloroform (MCF) in their CO inversion to provide a constraint on the OH abundance. However, MCF is observed at only a few surface sites, hence, although a MCF inversion might give a good global mean OH constraint, it will not help mitigate discrepancies in the regional distribution of OH. A better method to improve the OH would be to assimilate tropospheric ozone and its precursors, together with CO, as was done by Miyazaki et al. (2012). They showed that in such a multispecies assimilation, the adjustment in the monthly mean, zonal OH abundance could be as large as 20 %.

Our inversion results also highlight the need to better quantify the isoprene source of CO. Previous studies (e.g., Abbot et al., 2003; Shim et al., 2005; Millet et al., 2008) have used space-based observations of HCHO to infer isoprene emissions. Since

Sensitivity of inferred regional CO source estimates

Z. Jiang et al.

[Title Page](#)[Abstract](#)[Introduction](#)[Conclusions](#)[References](#)[Tables](#)[Figures](#)[Back](#)[Close](#)[Full Screen / Esc](#)[Printer-friendly Version](#)[Interactive Discussion](#)

Sensitivity of inferred regional CO source estimates

Z. Jiang et al.

Title Page

Abstract

Introduction

Conclusions

References

Tables

Figures



Back

Close

Full Screen / Esc

Printer-friendly Version

Interactive Discussion



rithm and selected results for the MOPITT instrument, *J. Geophys. Res.*, 108, 4399, doi:10.1029/2002JD003186, D14, 2003.

Deeter, M. N., Edwards, D. P., Gille, J. C., Emmons, L. K., Francis, G., Ho, S.-P., Mao, D., Masters, D., Worden, H., Drummond, J. R., and Novelli, P. C.: The MOPITT version 4 CO product: Algorithm enhancements, validation, and long-term stability, *J. Geophys. Res.*, 115, D07306, doi:10.1029/2009JD013005, 2010.

Deeter, M. N., Worden, H. M., Gille, J. C., Edwards, D. P., Mao, D., and Drummond, J. R.: MOPITT multispectral CO retrievals: Origins and effects of geophysical radiance errors, *J. Geophys. Res.*, 116, D15303, doi:10.1029/2011JD015703, 2011.

Deeter, M. N., Worden, H. M., Edwards, D. P., Gille, J. C., and Andrews, A. E.: Evaluation of MOPITT retrievals of lower-tropospheric carbon monoxide over the United States, *J. Geophys. Res.*, 117, D13306, doi:10.1029/2012JD017553, 2012.

Deeter, M. N., Martínez-Alonso, S., Edwards, D. P., Emmons, L. K., Gille, J. C., Worden, H. M., Pittman, J. V., Daube, B. C., and Wofsy, S. C.: Validation of MOPITT Version 5 thermal-infrared, near-infrared, and multispectral carbon monoxide profile retrievals for 2000–2011, *J. Geophys. Res. Atmos.*, 118, 6710–6725, doi:10.1002/jgrd.50272, 2013.

Evans, M. J., and Jacob, D. J.: Impact of new laboratory studies of N_2O_5 hydrolysis on global model budgets of tropospheric nitrogen oxides, ozone, and OH, *Geophys. Res. Lett.*, 32, L09813, doi:10.1029/2005GL022469, 2005.

Fortems-Cheiney, A., Chevallier, F., Pison, I., Bousquet, P., Szopa, S., Deeter, M. N., and Clerbaux, C.: Ten years of CO emissions as seen from Measurements of Pollution in the Troposphere (MOPITT), *J. Geophys. Res.*, 116, D05304, doi:10.1029/2010JD014416, 2011.

George, M., Clerbaux, C., Hurtmans, D., Turquety, S., Coheur, P.-F., Pommier, M., Hadji-Lazaro, J., Edwards, D. P., Worden, H., Luo, M., Rinsland, C., and McMillan, W.: Carbon monoxide distributions from the IASI/METOP mission: evaluation with other space-borne remote sensors, *Atmos. Chem. Phys.*, 9, 8317–8330, doi:10.5194/acp-9-8317-2009, 2009.

Gonzi, S., Feng, L., and Palmer, P. I.: Seasonal cycle of emissions of CO inferred from MOPITT profiles of CO: Sensitivity to pyroconvection and profile retrieval assumptions, *Geophys. Res. Lett.*, 38, L08813, doi:10.1029/2011GL046789, 2011.

Heald, C. L., Jacob, D. J., Jones, D. B. A., Palmer, P. I., Logan, J. A., Streets, D. G., Sachse, G. W., Gille, J. C., Hoffman, R. N., and Nehrkorn, T.: Comparative inverse analysis of satellite (MOPITT) and aircraft (TRACE-P) observations to estimate Asian sources of carbon monoxide, *J. Geophys. Res.* 109, D23306, doi:10.1029/2004JD005185, 2004.

Sensitivity of inferred regional CO source estimates

Z. Jiang et al.

Title Page

Abstract

Introduction

Conclusions

References

Tables

Figures



Back

Close

Full Screen / Esc

Printer-friendly Version

Interactive Discussion



- Henze, D. K., Hakami, A., and Seinfeld, J. H.: Development of the adjoint of GEOS- Chem, Atmos. Chem. Phys., 7, 2413–2433, doi:10.5194/acp-7-2413-2007, 2007.
- Henze, D. K., Seinfeld, J. H., and Shindell, D. T.: Inverse modeling and mapping US air quality influences of inorganic PM_{2.5} precursor emissions using the adjoint of GEOS-Chem, Atmos. Chem. Phys., 9, 5877–5903, doi:10.5194/acp-9-5877-2009, 2009.
- Hooghiemstra, Krol, M. C., Bergamaschi, P., de Laat, A. T. J., van der Werf, G. R., Novelli, P. C., Deeter, M. N., Aben, I., and Röckmann, T.: Comparing optimized CO emission estimates using MOPITT or NOAA surface network observations, J. Geophys. Res. 117, D06309, doi:10.1029/2011JD017043, 2012.
- Hudman, R. C., Murray, L. T., Jacob, D. J., Millet, D. B., Turquety, S., Wu, S., Blake, D. R., Goldstein, A. H., Holloway, J., and Sachse, G. W.: Biogenic versus anthropogenic sources of CO in the United States, Geophys. Res. Lett., 35, L04801, doi:10.1029/2007GL032393, 2008.
- Jiang, Z., D. Jones, B. A., Kopacz, M., Liu, J., Henze, D. K., and Heald, C., Quantifying the impact of model errors on top-down estimates of carbon monoxide emissions using satellite observations, J. Geophys. Res., 116, D15306, doi:10.1029/2010JD015282, 2011.
- Jiang, Z., Jones, D. B. A., Worden, H. M., Deeter, M. N., Henze, D. K., Worden, J., Bowman, K. W., Brenninkmeijer, C. A. M., and Schuck, T. J.: Impact of model errors in convective transport on CO source estimates inferred from MOPITT CO retrievals, J. Geophys. Res. Atmos., 118, 2073–2083, doi:10.1002/jgrd.50216, 2013.
- Jiang, Z., Jones, D. B. A., Henze, D., Worden, H., Wang, Y. X.: Regional data assimilation of multi-spectral MOPITT observations of CO over North America, submitted to Atmos. Chem. Phys. Discuss., 2014.
- Jones, D. B. A., Bowman, K. W., Logan, J. A., Heald, C. L., Liu, J., Luo, M., Worden, J., and Drummond, J.: The zonal structure of tropical O₃ and CO as observed by the Tropospheric Emission Spectrometer in November 2004 – Part 1: Inverse modeling of CO emissions, Atmos. Chem. Phys., 9, 3547–3562, doi:10.5194/acp-9-3547-2009, 2009.
- Kopacz, M., Jacob, D. J., Henze, D. K., Heald, C. L., Streets, D. G., and Zhang, Q.: Comparison of adjoint and analytical Bayesian inversion methods for constraining Asian sources of carbon monoxide using satellite (MOPITT) measurements of CO columns, J. Geophys. Res., 114, D04305, doi:10.1029/2007JD009264, 2009.
- Kopacz, M., Jacob, D. J., Fisher, J. A., Logan, J. A., Zhang, L., Megretskaia, I. A., Yantosca, R. M., Singh, K., Henze, D. K., Burrows, J. P., Buchwitz, M., Khlystova, I., McMillan, W.

Sensitivity of inferred regional CO source estimates

Z. Jiang et al.

[Title Page](#)[Abstract](#)[Introduction](#)[Conclusions](#)[References](#)[Tables](#)[Figures](#)[Back](#)[Close](#)[Full Screen / Esc](#)[Printer-friendly Version](#)[Interactive Discussion](#)

W., Gille, J. C., Edwards, D. P., Eldering, A., Thouret, V. and Nedelec, P.: Global estimates of CO sources with high resolution by adjoint inversion of multiple satellite datasets (MOPITT, AIRS, SCIAMACHY, TES), *Atmos. Chem. Phys.*, 10, 855–876, doi:10.5194/acp-10-855-2010, 2010.

5 Kuhn, H., Green, M., and Etyemezian, V.: Big Bend Regional Aerosol and Visibility Observational (BRAVO) Study Emissions Inventory, Report prepared for BRAVO Steering Committee, Desert Research Institute, Las Vegas, Nevada, 2003.

Liu, J.-H., Logan, J. A., Jones, D. B. A., Livesey, N. J., Megretskaia, I., Carouge, C. and Nedelec, P.: Analysis of CO in the tropical troposphere using Aura satellite data and the GEOS-Chem model: insights into transport characteristics of the GEOS meteorological products, *Atmos. Chem. Phys.*, 10, 12207–12232, doi:10.5194/acp-10-12207-2010, 2010.

10 Luo, M., Rinsland, C. P., Rodgers, C. D., Logan, J. A., Worden, H., Kulawik, S., Eldering, A., Goldman, A., Shephard, M. W., Gunson, M., and Lampel, M.: Comparison of carbon monoxide measurements by TES and MOPITT: The influence of a priori data and instrument characteristics on nadir atmospheric species retrievals, *J. Geophys. Res.*, 112, D09303, doi:10.1029/2006JD007663, 2007.

15 Millet, D. B., Jacob, D. J., Boersma, K. F., Fu, T.-M., Kurosu, T. P., Chance, K., Heald, C. L., Guenther, A.: Spatial distribution of isoprene emissions from North America derived from formaldehyde column measurements by the OMI satellite sensor, *J. Geophys. Res.*, 113, D02307, doi:10.1029/2007JD008950, 2008.

20 Miyazaki, K., Eskes, H. J., Sudo, K., Takigawa, M., van Weele, M., and Boersma, K. F.: Simultaneous assimilation of satellite NO₂, O₃, CO, and HNO₃ data for the analysis of tropospheric chemical composition and emissions, *Atmos. Chem. Phys.*, 12, 9545–9579, doi:10.5194/acp-12-9545-2012, 2012.

25 Olivier, J. G. J. and Berdowski, J. J. M.: Global emissions sources and sinks, in: *The Climate System*, edited by: Berdowski, J., Guicherit, R., and Heij, B. J., 33–78, A. A. Balkema Publishers/Swets & Zeitlinger Publishers, Lisse, the Netherlands, 2001.

30 Palmer, P. I., Jacob, D. J., Jones, D. B. A., Heald, C. L., Yantosca, R. M., Logan, J. A., Sachse, G. W., and Streets, D. G.: Inverting for emissions of carbon monoxide from Asia using aircraft observations over the western Pacific, *J. Geophys. Res.*, 108, 8828, doi:10.1029/2003JD003397, 2003.

Sensitivity of inferred regional CO source estimates

Z. Jiang et al.

Title Page

Abstract

Introduction

Conclusions

References

Tables

Figures



Back

Close

Full Screen / Esc

Printer-friendly Version

Interactive Discussion



- Palmer, P. I., Suntharalingam, P., Jones, D. B. A., Jacob, D. J., Streets, D. G., Fu, Q., Vay, S. A., and Sachse, G. W.: Using CO₂:CO correlations to improve inverse analyses of carbon fluxes, *J. Geophys. Res.*, 111, D12318, doi:10.1029/2005JD006697, 2006.
- Parrington, M., Jones, D. B. A., Bowman, K. W., Horowitz, L. W., Thompson, A. M., Tarasick, D. W., and Witte, J. C.: Estimating the summertime tropospheric ozone distribution over North America through assimilation of observations from the Tropospheric Emission Spectrometer, *J. Geophys. Res.*, 113, D18307, doi:10.1029/2007JD009341, 2008.
- Parrington, M., Palmer, P. I., Henze, D. K., Tarasick, D. W., Hyer, E. J., Owen, R. C., Helmig, D., Clerbaux, C., Bowman, K. W., Deeter, M. N., Barratt, E. M., Coheur, P.-F., Hurtmans, D., Jiang, Z., George, M., and Worden, J. R.: The influence of boreal biomass burning emissions on the distribution of tropospheric ozone over North America and the North Atlantic during 2010, *Atmos. Chem. Phys.*, 12, 2077–2098, doi:10.5194/acp-12-2077-2012, 2012.
- Pétron, G., Granier, C., Khatatov, B., Yudin, V., Lamarque, J.-F., Emmons, L., Gille, J., and Edwards, D. P.: Monthly CO surface sources inventory based on the 2000–2001 MOPITT satellite data, *Geophys. Res. Lett.*, 31, L21107, doi:10.1029/2004GL020560, 2004.
- Shim, C., Wang, Y.-H., Choi, Y., Palmer, P. I., Abbot, D. S., and Chance, K.: Constraining global isoprene emissions with Global Ozone Monitoring Experiment (GOME) formaldehyde column measurements, *J. Geophys. Res.*, 110, D24301, doi:10.1029/2004JD005629, 2005.
- Shindell, D. T., Faluvegi, G., Stevenson, D. S., Krol, M. C., Emmons, L. K., Lamarque, J.-F., Petron, G., Dentener, F. J., Ellingsen, K., Schultz, M. G., Wild, O., Amann, M., Atherton, C. S., Bergmann, D. J., Bey, I., Butler, T., Cofala, J., Collins, W. J., Derwent, R. G., Doherty, R. M., Drevet, J., Eskes, H. J., Fiore, A. M., Gauss, M., Hauglustaine, D. A., Horowitz, L. W., Isaksen, S. A., Lawrence, M. G., Montanaro, V., Müller, J.-F., Pitari, G., Parther, M. J., Pyle, J. A., Rast, S., Rodriguez, J. M., Sanderson, M. G., Savage, N. H., Strahan, S. E., Sudo, K., Szopa, S., Unger, N., van Noije, T. P. C. and Zeng, G.: Multimodel simulations of carbon monoxide: Comparison with observations and projected near-future changes, *J. Geophys. Res.*, 111, D19306, doi:10.1029/2006JD007100, 2006.
- Singh, K., Jardak, M., Sandu, A., Bowman, K., Lee, M., and Jones, D.: Construction of non-diagonal background error covariance matrices for global chemical data assimilation, *Geosci. Model Dev.*, 4, 299–316, doi:10.5194/gmd-4-299-2011, 2011.
- Spivakovsky, C. M., Logan, J. A., Montzka, S. A., Balkanski, Y. J., Foreman-Fowler, M., Jones, D. B. A., Horowitz, L. W., Fusco, A. C., Brenninkmeijer, C. A. M., Prather, M. J., Wofsy, S. C.,

Sensitivity of inferred regional CO source estimates

Z. Jiang et al.

Title Page

Abstract

Introduction

Conclusions

References

Tables

Figures



Back

Close

Full Screen / Esc

Printer-friendly Version

Interactive Discussion



and McElroy, M. B.: Three-dimensional climatological distribution of tropospheric OH Update and evaluation, *J. Geophys. Res.*, 105, 8931–8980, doi:10.1029/1999JD901006, 2000.

5 Staudt, A. C., Jacob, D. J., Logan, J. A., Bachiochi, D., Krishnamurti, T. N., and Poisson, N.: Global chemical model analysis of biomass burning and lightning influences over the South Pacific in austral spring, *J. Geophys. Res.*, 107, ACH 11-1–ACH 11-17, doi:10.1029/2000JD000296, 2002.

Vestreng, V. and Klein, H.: Emission data reported to UNECE/EMEP. Quality assurance and trend analysis and Presentation of WebDab, Norwegian Meteorological Institute, Oslo, Norway, MSC-W Status Report, 2002.

10 van der Werf, G. R., Randerson, J. T., Giglio, L., Collatz, G. J., Mu, M., Kasibhatla, P. S., Morton, D. C., DeFries, R. S., Jin, Y., and van Leeuwen, T. T.: Global fire emissions and the contribution of deforestation, savanna, forest, agricultural, and peat fires (1997–2009), *Atmos. Chem. Phys.*, 10, 11707–11735, doi:10.5194/acp-10-11707-2010, 2010.

15 Wang, H., Jacob, D. J., Kopacz, M., Jones, D. B. A., Suntharalingam, P., Fisher, J. A., Nassar, R., Pawson, S., and Nielsen, J. E.: Error correlation between CO₂ and CO as constraint for CO₂ flux inversions using satellite data, *Atmos. Chem. Phys.*, 9, 7313–7323, doi:10.5194/acp-9-7313-2009, 2009.

20 Warner, J., Comer, M. M., Barnett, C. D., McMillan, W. Wolf, W., Maddy, W., E., and Sachse, G.: A comparison of satellite tropospheric carbon monoxide measurements from AIRS and MOPITT during INTEX-NA, *J. Geophys. Res.*, 112, D12S17, doi:10.1029/2006JD007925, 2007.

Worden, H. M., Deeter, M. N., Edwards, D. P., Gille, J. C., Drummond, J. R., and Nédélec, P.: Observations of near-surface carbon monoxide from space using MOPITT multispectral retrievals, *J. Geophys. Res.*, 115, D18314, doi:10.1029/2010JD014242, 2010.

25 Worden, J., Jiang, Z., Jones, D. B. A., Alvarado, M., Bowman, K., Frankenberg, C., Kort, E. A., Kulawik, S. S., Lee, M.-M., Liu, J.-J., Payne, V., Wecht, K. and Worden, H.: El Nino, The 2006 Indonesian Peat Fires, And The Distribution Of Atmospheric Methane, *Geophys. Res. Lett.*, 40, 4938–4943, doi:10.1002/grl.50937, 2013.

30 Zhang, Q., Streets, D. G., Carmichael, G. R., He, K. B., Huo, H., Kannari, A., Klimont, Z., Park, I. S., Reddy, S., Fu, J. S., Chen, D., Duan, L., Lei, Y., Wang, L. T., and Yao, Z. L.: Asian emissions in 2006 for the NASA INTEX-B mission, *Atmos. Chem. Phys.*, 9, 5131–5153, doi:10.5194/acp-9-5131-2009, 2009.

Sensitivity of inferred regional CO source estimates

Z. Jiang et al.

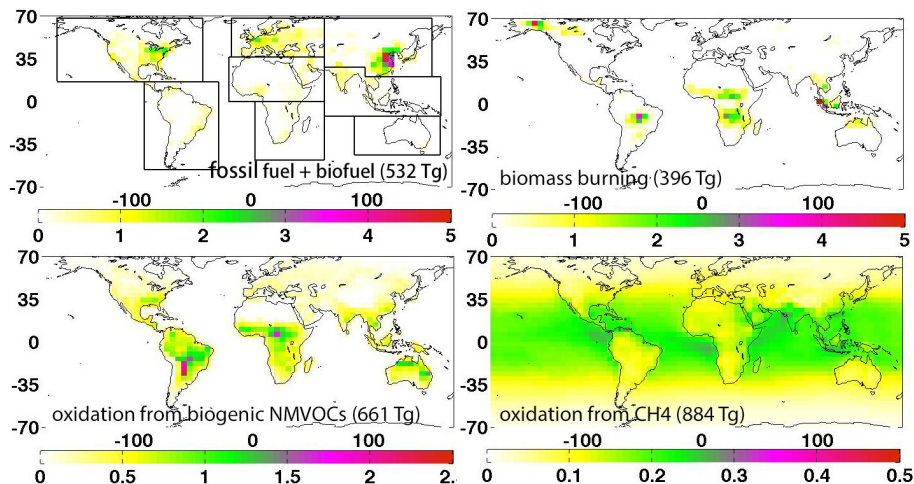


Figure 1. Annual mean CO emissions from combustion sources and the oxidation of biogenic NMVOC and CH₄, averaged from June 2004 to May 2005. The unit is 10^{12} molec cm⁻² s⁻¹. The continental domains are defined with black boxes. The sub-continental domains in North America (US, Mexico, Alaska and Canada) are separated based on the country boundaries.

Title Page

Abstract

Introduction

Conclusions

References

Tables

Figures



Back

Close

Full Screen / Esc

Printer-friendly Version

Interactive Discussion



Sensitivity of inferred regional CO source estimates

Z. Jiang et al.

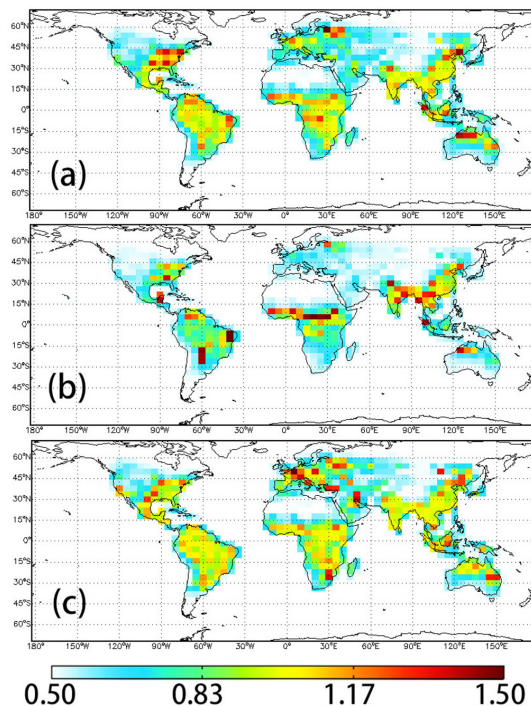


Figure 2. OSSE scaling factors for April 2006. The scaling factors represent the ratio of the estimated to true emissions. The ratio for the first guess is 0.5. The actual value is 1.0. Shown are the scaling factors obtained with: **(a)** the linear scaling factor optimization, **(b)** the LOG scaling factor optimization, **(c)** the LOGX2 scaling factor optimization.

Title Page

Abstract

Introduction

Conclusions

References

Tables

Figures

◀

▶

◀

▶

Back

Close

Full Screen / Esc

Printer-friendly Version

Interactive Discussion



Sensitivity of inferred regional CO source estimates

Z. Jiang et al.

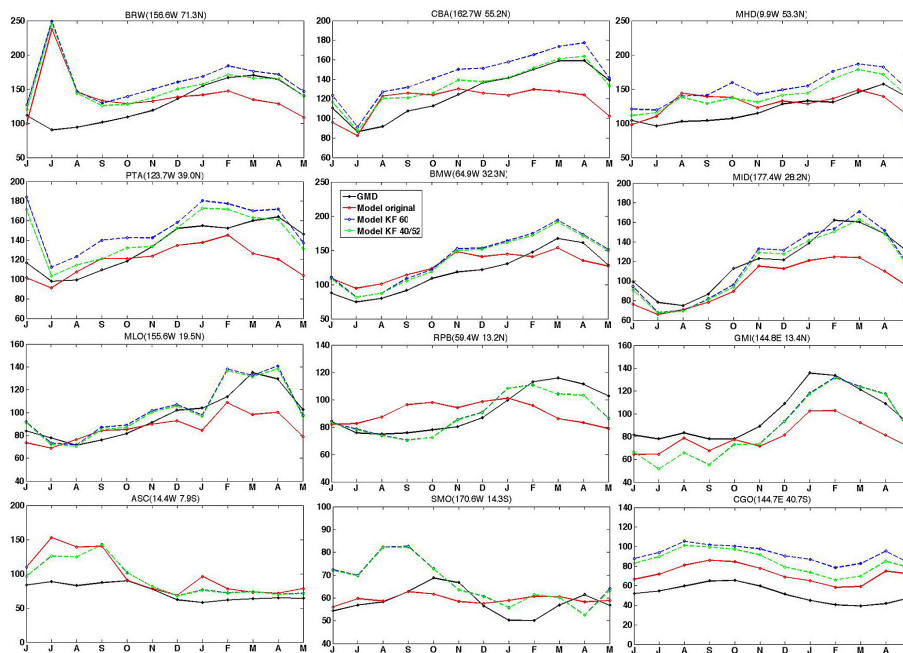


Figure 3. Annual variation of monthly mean CO concentration at selected GMD sites. Black solid line shows the GMD monthly mean CO. Red solid line shows the free model simulation with original initial condition. The blue dash line is the assimilation result using MOPITT from 60° S to 60° N. The green dash line is the assimilation result from excluding the high latitude data.

Title Page

Abstract

Introduction

Conclusions

References

Tables

Figures



Back

Close

Full Screen / Esc

Printer-friendly Version

Interactive Discussion



Sensitivity of inferred regional CO source estimates

Z. Jiang et al.

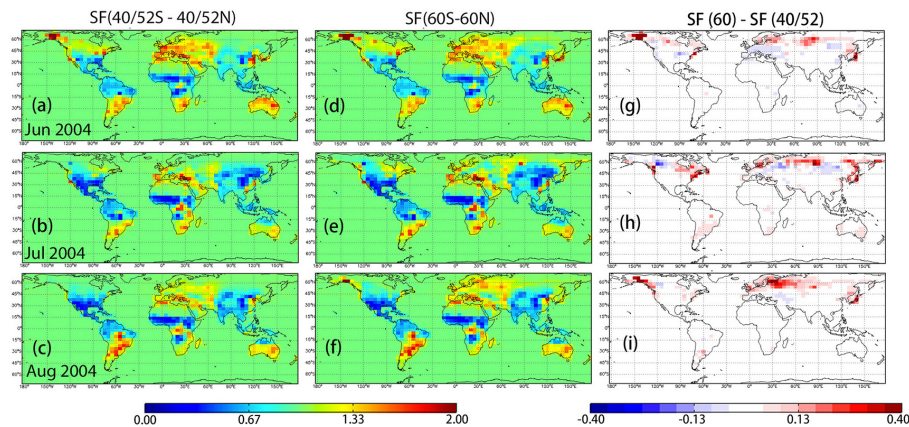


Figure 4. (a)–(c) Scaling factors without high latitude MOPITT data. (d)–(f) scaling factors with high latitude MOPITT data. (g)–(i) difference between two types of scaling factors.

[Title Page](#)[Abstract](#)[Introduction](#)[Conclusions](#)[References](#)[Tables](#)[Figures](#)[Back](#)[Close](#)[Full Screen / Esc](#)[Printer-friendly Version](#)[Interactive Discussion](#)

Sensitivity of inferred regional CO source estimates

Z. Jiang et al.

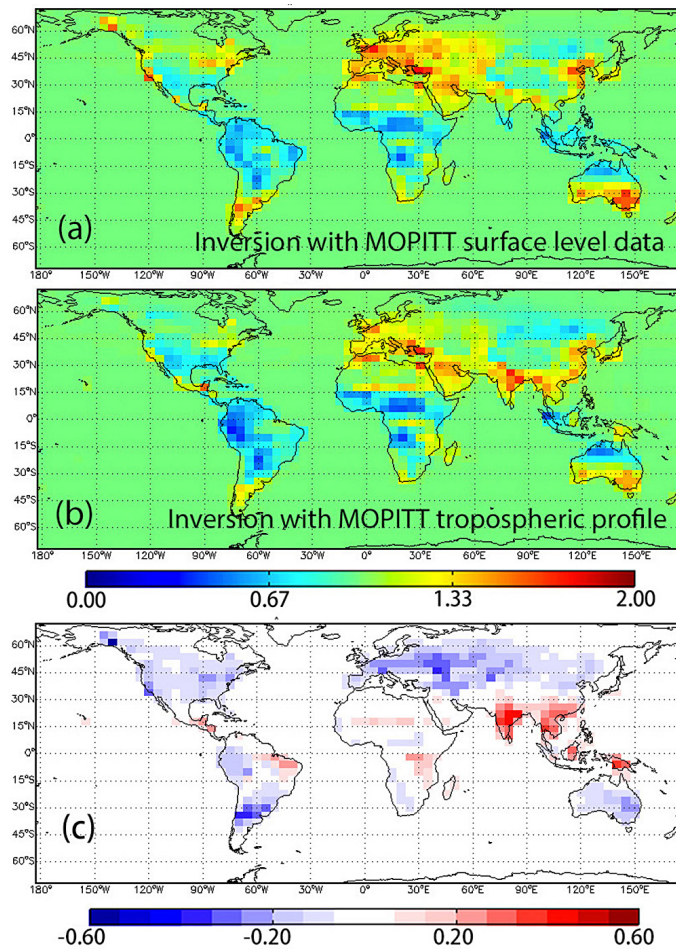


Figure 5. (a) Annual mean scaling factors, from June 2004 to May 2005, using MOPITT V5J surface level and (b) tropospheric profile data. (c) Difference between two scaling factors.

Sensitivity of inferred regional CO source estimates

Z. Jiang et al.

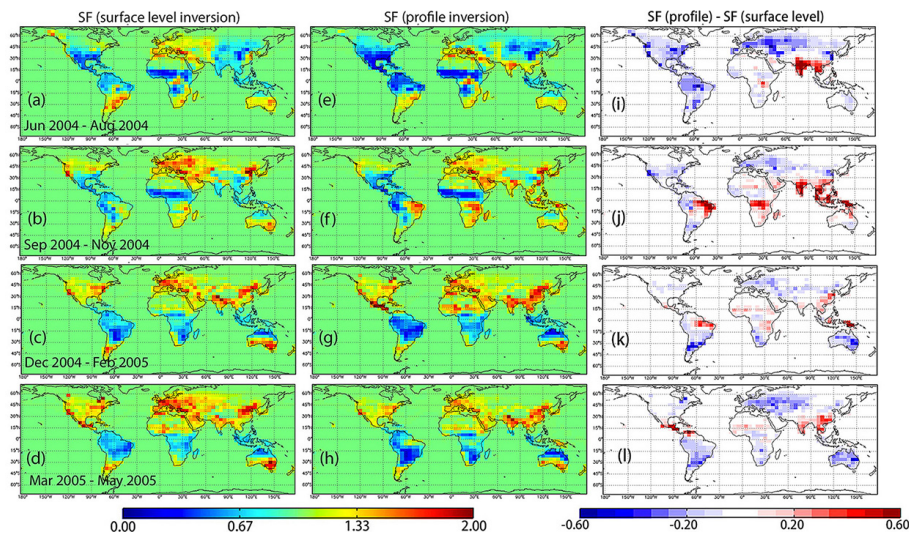


Figure 6. (a)–(d) seasonal mean scaling factors, using MOPITT V5J surface level data; (e)–(h) seasonal mean scaling factors, using MOPITT V5J tropospheric profile data; (i)–(l) difference between two scaling factors.

Title Page	
Abstract	Introduction
Conclusions	References
Tables	Figures
◀	▶
◀	▶
Back	Close
Full Screen / Esc	
Printer-friendly Version	
Interactive Discussion	



Sensitivity of inferred regional CO source estimates

Z. Jiang et al.

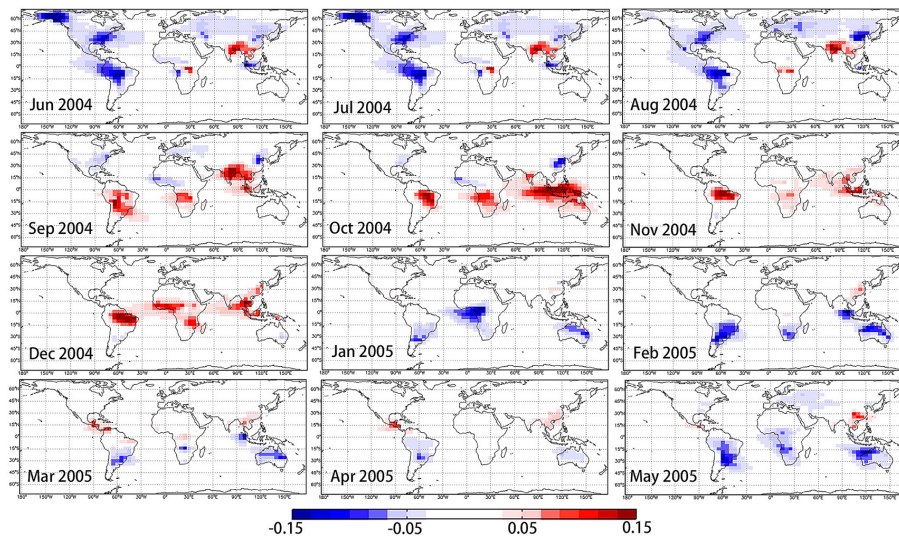


Figure 8. Relative difference of monthly mean tropospheric CO column, calculated as $2(\text{CO}_{\text{profile}} - \text{CO}_{\text{surface}}) / (\text{CO}_{\text{profile}} + \text{CO}_{\text{surface}})$.

[Title Page](#)[Abstract](#)[Introduction](#)[Conclusions](#)[References](#)[Tables](#)[Figures](#)[Back](#)[Close](#)[Full Screen / Esc](#)[Printer-friendly Version](#)[Interactive Discussion](#)

Sensitivity of inferred regional CO source estimates

Z. Jiang et al.

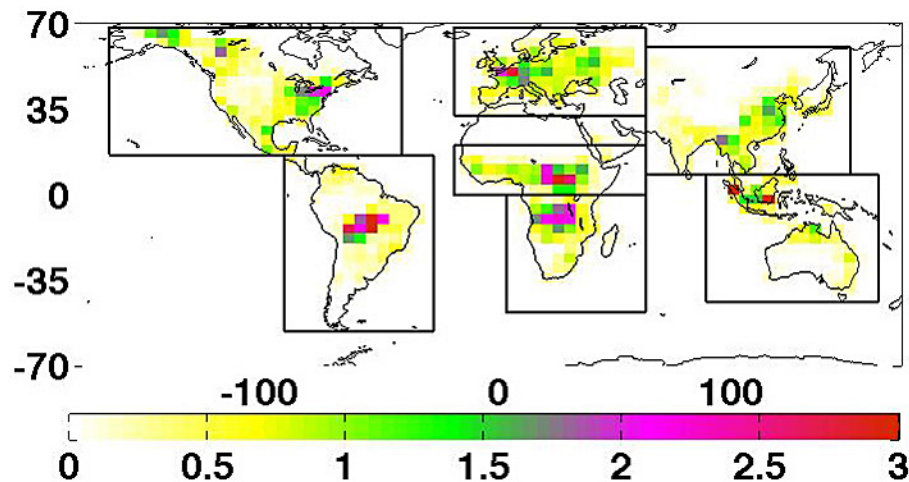


Figure 9. Distribution of emissions used for the idealized 30-day tracer. The unit is $10^{13} \text{ molec cm}^{-2} \text{ s}^{-1}$.

[Title Page](#)[Abstract](#)[Introduction](#)[Conclusions](#)[References](#)[Tables](#)[Figures](#)[◀](#)[▶](#)[◀](#)[▶](#)[Back](#)[Close](#)[Full Screen / Esc](#)[Printer-friendly Version](#)[Interactive Discussion](#)

Sensitivity of inferred regional CO source estimates

Z. Jiang et al.

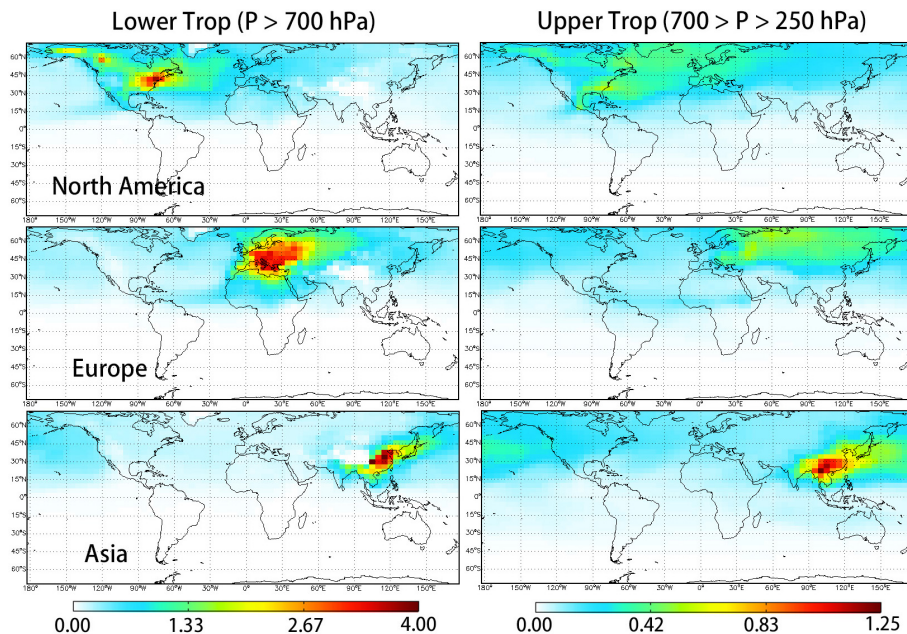


Figure 10a. 30-day tracer partial columns in the extratropics for June 2004. Note the difference in scales between the lower and upper tropospheric columns.

[Title Page](#)[Abstract](#)[Introduction](#)[Conclusions](#)[References](#)[Tables](#)[Figures](#)[◀](#)[▶](#)[◀](#)[▶](#)[Back](#)[Close](#)[Full Screen / Esc](#)[Printer-friendly Version](#)[Interactive Discussion](#)

Sensitivity of inferred regional CO source estimates

Z. Jiang et al.

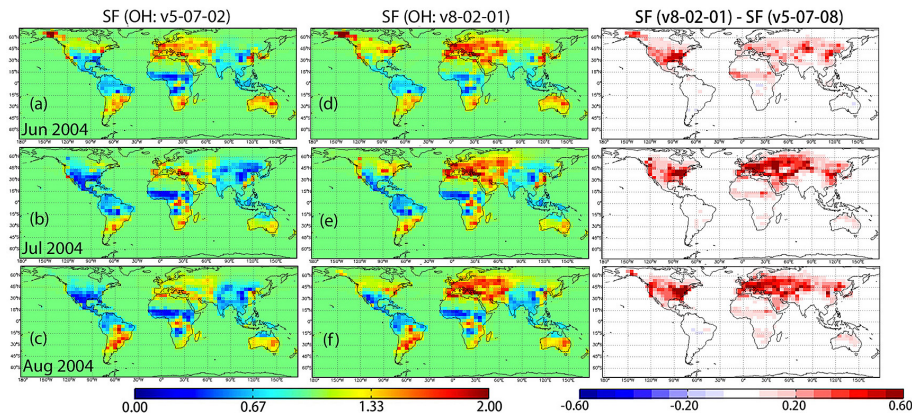


Figure 12. Scaling factors with MOPITT surface level retrievals and their difference. **(a)–(c)** Scaling factors, using v5-07-08 OH; **(d)–(f)** Scaling factors, using v8-02-01 OH; **(i)–(l)** Difference between two scaling factors.

Title Page

Abstract

Introduction

Conclusions

References

Tables

Figures



Back

Close

Full Screen / Esc

Printer-friendly Version

Interactive Discussion



Sensitivity of inferred regional CO source estimates

Z. Jiang et al.

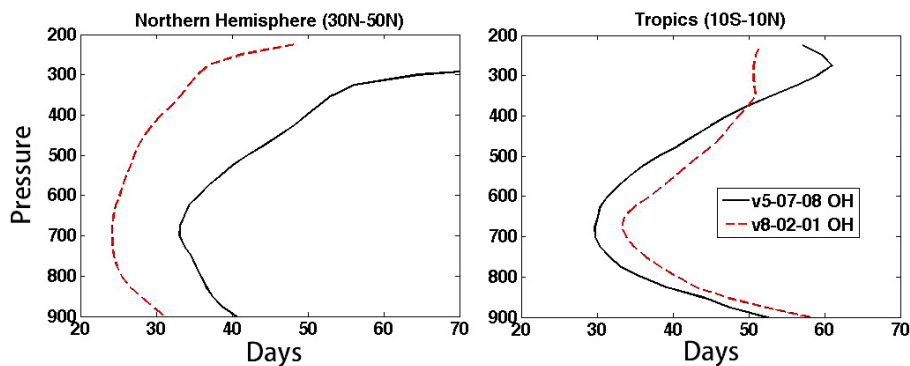


Figure 13. Atmospheric CO lifetime averaged zonally at 30N-50N and 10S-10N for August 2004, estimated using v5-07-08 (black solid line) and v8-02-01 (red dash line) OH fields.

[Title Page](#)[Abstract](#)[Introduction](#)[Conclusions](#)[References](#)[Tables](#)[Figures](#)[◀](#)[▶](#)[◀](#)[▶](#)[Back](#)[Close](#)[Full Screen / Esc](#)[Printer-friendly Version](#)[Interactive Discussion](#)

Sensitivity of inferred regional CO source estimates

Z. Jiang et al.

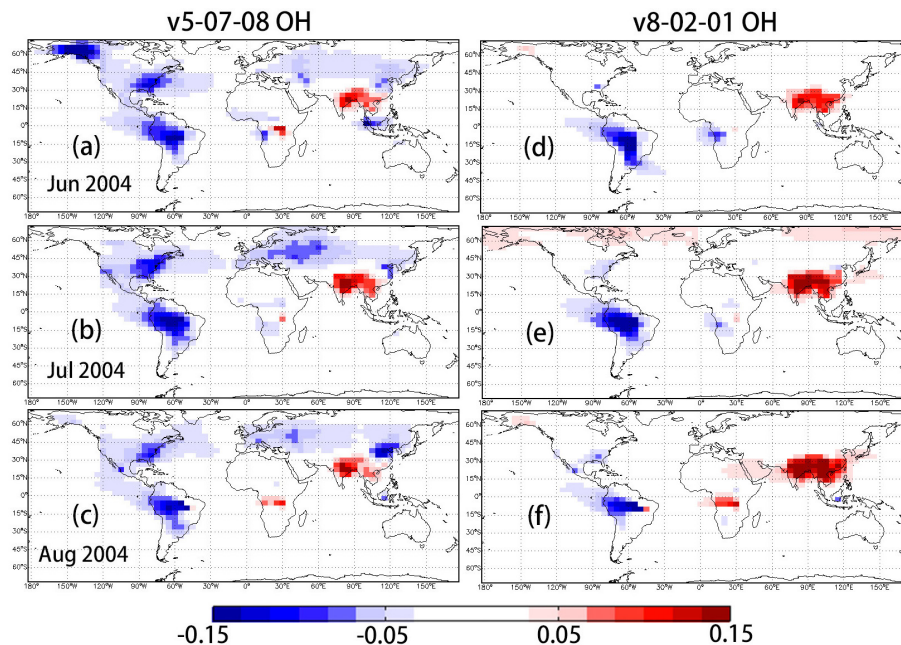


Figure 14. Relative difference of monthly mean tropospheric CO column, calculated as $2(\text{CO_profile} - \text{CO_surface}) / (\text{CO_profile} + \text{CO_surface})$. (a)–(c) with v5-07-02 OH; (d)–(f) with v8-02-01 OH.

[Title Page](#)[Abstract](#)[Introduction](#)[Conclusions](#)[References](#)[Tables](#)[Figures](#)[◀](#)[▶](#)[◀](#)[▶](#)[Back](#)[Close](#)[Full Screen / Esc](#)[Printer-friendly Version](#)[Interactive Discussion](#)